Biomatter 4, e28536; March 2014; © 2014 Landes Bioscience

The role of dialysis and freezing on structural conformation, thermal properties and morphology of silk fibroin hydrogels

Marta Ribeiro[1,2,*], Mariana A de Moraes[3], Marisa M Beppu[3], Fernando J Monteiro[1,2], and Maria P Ferraz[1,4]

[1]Instituto de Engenharia Biomédica; Universidade do Porto; Porto, Portugal; [2]Departamento de Engenharia Metalúrgica e Materiais; Universidade do Porto; Porto, Portugal; [3]Faculdade de Engenharia Química; Universidade Estadual de Campinas; Campinas, Brasil; [4]Centro de Estudos em Biomedicina; Universidade Fernando Pessoa; Porto, Portugal

Keywords: biomaterials; biopolymer; silk fibroin; gelation; scaffold

Silk fibroin has been widely explored for many biomedical applications, due to its biocompatibility and biodegradability. The aim of this work was to study the role of dialysis and freezing on structural conformation, thermal properties and morphology of silk fibroin hydrogels. Hydrogels were prepared after 3 and 7 days of dialysis and the effect of freezing was analyzed. For that purpose, a part of the fibroin hydrogels underwent freezing at -20 °C for 24 h, followed by lyophilization and the rest of the hydrogels were kept at 8 °C for 24 h, with further lyophilization. The fibroin hydrogels were characterized by X-ray diffraction (XRD), Fourier transformed infrared spectroscopy (FTIR), thermogravimetric analysis (TGA) and scanning electron microscopy (SEM). Measurements by XRD and FTIR indicated that silk I and silk II structures were present in the fibroin hydrogels and that the secondary structure of fibroin is transformed mostly to β-sheet during the gelation process. Thermal analysis indicated that fibroin hydrogels are thermally stable with the degradation peak at around 330–340 °C. SEM micrographs showed porous structures and the fibroin hydrogels subjected to freezing presented a much larger pore size. Results indicate that the dialysis time and freezing did not alter the material crystallinity, conformation or thermal behavior; however, hydrogel microstructure was strongly affected by dialysis time and freezing, showing controlled pores size. This study provides fundamental knowledge on silk fibroin hydrogels preparation and properties and the studied hydrogels are promising to be used in the biomaterial field.

Introduction

Replacement of functional tissues requires the development of three-dimensional (3D) scaffolds that can provide an optimum microenvironment for tissue growth and regeneration.[1,2] Pore architecture in 3D polymeric scaffolds is known to play a critical role in tissue engineering as it provides the growth, adhesion, migration and proliferation of cells. Therefore, the scaffolds should have suitable properties such as interconnecting network of pores for the effective migration, growth and attachment of cells, sufficient porosity for the effective transport of nutrients and waste, biocompatibility, and biodegradation properties, for being exploited in tissue engineering applications.[3]

Silk fibroin (SF) derived from *Bombyx mori* silkworm is a structural protein which possesses many important properties for tissue engineering and regenerative medicine, such as versatile processing, slow biodegradation, good biocompatibility, low immunogenicity, low inflammatory response, adjustable mechanical properties, high permeability to oxygen and water vapor and resistance to enzymatic degradation.[4-6]

The cocoon of the silkworm is mainly composed of two protein components, fibroin and sericin. Fibroin is the water insoluble structural protein component of silk fibers whereas sericin is the water-soluble glue-like protein that holds SF fibers together.[4] Since the sericin contamination was identified to be the main source of problems, such as unwanted immunological reactions in vivo,[7,8] purified SF has become a novel, promising biomaterial and has found increasing numbers of applications in clinical devices including in tissue engineering of cartilage, bone, muscle, ligament and tendon tissues.[9-13] Fibroin is the core protein which accounts for 70% of the cocoon and is a hydrophobic glycoprotein.[4] SF consists mainly of the amino acids glycine, alanine and serine which form antiparallel β-sheets in the spun fibers and provide stability and interesting mechanical properties to the fibers.[4,14] SF can assume distinct conformations; α-helix and random-coil conformations (also called silk I) and the β-sheet conformation (silk II). Silk I is a metastable form that is soluble in water and silk II is insoluble in water and is the most stable structure, where SF chains are connected by hydrogen bonds between the adjacent segments of polypeptide chains.[5,15-17]

SF fibers, extracted from *B. mori* cocoons, are insoluble in water and in the majority of organic solvents. SF dissolves in concentrated acid solutions and in concentrated aqueous, organic and aqueous-organic salts solutions.[18] These solutions contain

*Correspondence to: ribeiro_marta88@hotmail.com
Submitted: 12/05/2013; Revised: 02/26/2014; Accepted: 03/14/2014; Published Online: 03/19/2014
Citation: Ribeiro M, de Moraes MA, Beppu MM, Monteiro FJ, Ferraz MP. The role of dialysis and freezing on structural conformation, thermal properties and morphology of silk fibroin hydrogels. Biomatter 2014; 4:e28536; PMID: 24646905; http://dx.doi.org/10.4161/biom.28536

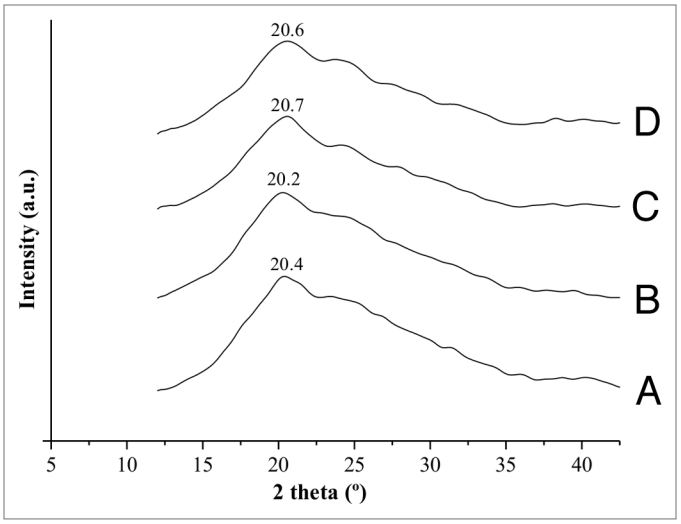

Figure 1. X-ray diffractograms of SF hydrogels formed at 37 °C after 3 d of dialysis subjected to freezing (**A**) or kept at 8 °C (**B**) and SF hydrogels formed after 7 d of dialysis subjected to freezing (**C**) or kept at 8 °C (**D**).

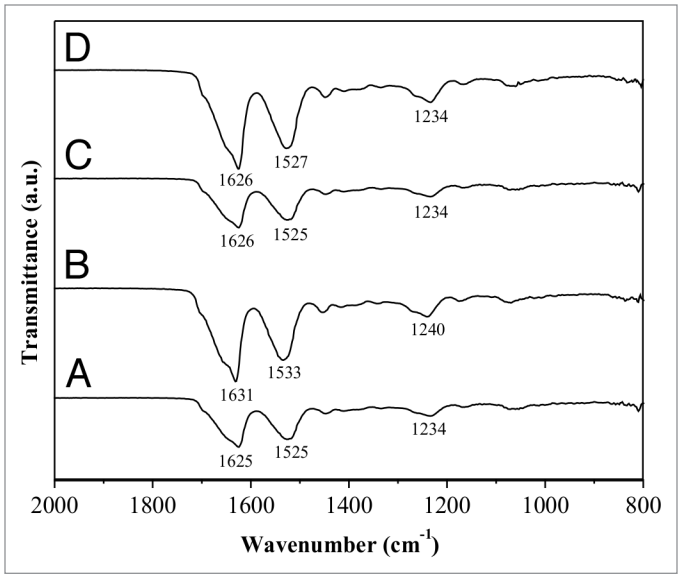

Figure 2. FTIR-ATR spectra of SF hydrogels formed at 37 °C after 3 d of dialysis subjected to freezing (**A**) or kept at 8 °C (**B**) and SF hydrogels formed after 7 d of dialysis subjected to freezing (**C**) or kept at 8 °C (**D**).

highly concentrated salts that need to be removed by dialysis in order to prepare SF-based materials, such as hydrogels,[19] films[17] and nanoparticles.[20] SF solution after dialysis is metastable (predominance of silk I) and it can easily convert to a more stable form, by a conformational transition to silk II, forming stable hydrogels. SF gelation from aqueous solution is a kinetic process and depends on factors such as SF concentration, temperature, pH[21] and presence of other materials, such as poly(*N*-isopropylacrylamide)[22] and poly(ethylene oxide) polymers[23]. SF gelation process is also influenced by dialysis parameters, since the rate of salt removal will directly influence the conformational transition of SF. The rate of salt removal can influence SF conformational transition, since the salt is responsible for SF solvation and stabilization in solution. When salt is removed, a metastable solution is obtained and at this point gelation is just a kinetic process. If the necessary amount of salt is not removed during dialysis, SF-based materials cannot be prepared due to the strong salt solvation. On the contrary, the more salt is removed, the more rapid is the gelation process.[19] Thus, dialysis is a key parameter on SF gelation and the study of dialysis time is important to define SF hydrogels properties.

Cryogenic processes, based on freezing of hydrogels, and subsequent lyophilization, are widely used for scaffold preparation because of the biocompatibility of both the template and the process for template removal.[24-26] During the freezing step, solvent crystals grow at a controllable rate and solute molecules are excluded from the frozen solvent until the sample is completely frozen. The freezing step is very important in order to produce desirable porous structures, with control over the pores size and quantity, depending on parameters such as freezing temperature and rate.[27]

The purpose of the present study was to study the role of dialysis and freezing on structural conformation, thermal properties and morphology of silk fibroin hydrogels. Hydrogels were prepared after 3 and 7 d of dialysis and the effect of freezing was analyzed. The structure and properties of SF hydrogels were determined by X-ray diffraction (XRD), Fourier transformed infrared spectroscopy (FTIR), thermogravimetric analysis (TGA) and scanning electron microscopy (SEM).

Results

Crystallinity

Figure 1 shows the X-ray diffractograms of SF hydrogels prepared from SF solution subjected to different dialysis time and freezing. The halos at 2θ = 20.4°, 2θ = 20.2°, 2θ = 20.7° and 2θ = 20.6° appearing in the XRD spectra of SF hydrogels formed at 37 °C after 3 d of dialysis subjected to freezing (**Fig. 1A**), SF hydrogels formed at 37 °C after 3 d of dialysis kept at 8 °C (**Fig. 1B**), SF hydrogels formed at 37 °C after 7 d of dialysis subjected to freezing (**Fig. 1C**) and SF hydrogels formed at 37 °C after 7 d of dialysis kept at 8 °C (**Fig. 1D**), respectively, are attributed to the silk II (β-sheet) conformation.[14,20,28-30]

Structural conformation

By analyzing the infrared spectrum, the structural conformation of SF can be determined, depending on the wavenumber location of the absorption bands of amides I, II and III. Amide I, II, and III bands are attributed to C = O stretching, N-H deformation, and O-C-N bending, respectively.[31]

The infrared spectra of the SF hydrogels are shown in **Figure 2**. The SF hydrogel formed at 37 °C after 3 d of dialysis and subjected to freezing (**Fig. 2A**) presented absorption bands at 1625 cm^{-1} (amide I) and 1525 cm^{-1} (amide II), corresponding to the silk II structural conformation.[32-34] Other adsorption band was observed at 1234 cm^{-1} (amide III), which is characteristic of the silk I conformation.[35]

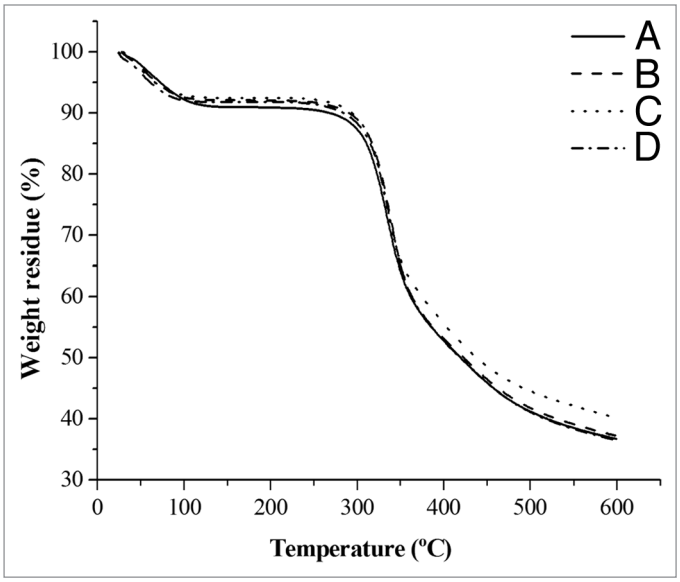

Figure 3. TGA curves of SF hydrogels formed at 37 °C after 3 d of dialysis subjected to freezing (**A**) or kept at 8 °C (**B**) and SF hydrogels formed after 7 d of dialysis subjected to freezing (**C**) or kept at 8 °C (**D**).

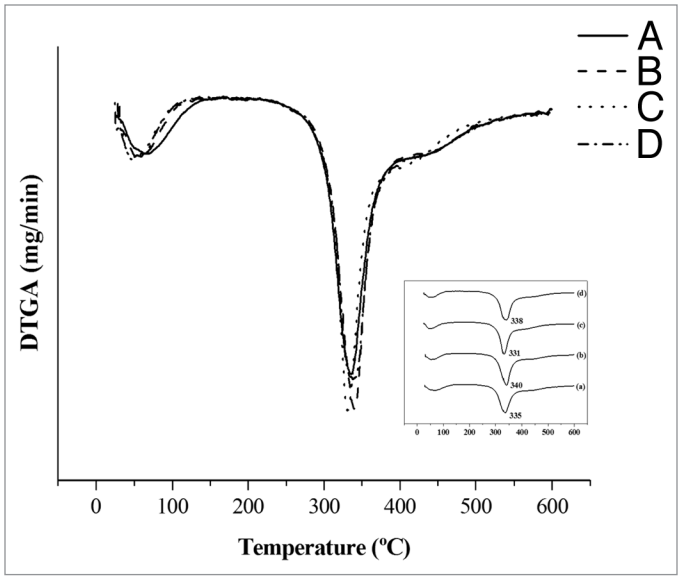

Figure 4. DTGA wide scan curves of SF hydrogels and detected degradation peaks (inset) in all hydrogels. SF hydrogels formed at 37 °C after 3 d of dialysis subjected to freezing (**A**) or kept at 8 °C (**B**) and SF hydrogels formed after 7 d of dialysis subjected to freezing (**C**) or kept at 8 °C (**D**).

The SF hydrogel formed at 37 °C after 3 d of dialysis and kept at 8 °C (**Fig. 2B**) showed adsorption bands at 1631 cm^{-1} (amide I) and 1533 cm^{-1} (amide II), indicating the existence of the silk II structural conformation.[32-34] The adsorption band at 1240 cm^{-1} (amide III) is characteristic of the silk I conformation.[36]

The SF hydrogels formed after 7 d of dialysis subjected to freezing or not (**Fig. 2C and D**, respectively) presented similar spectra, with adsorption band at 1635 cm^{-1} (amide I) corresponding to the SF silk II structural conformation.[32-34] The adsorption bands at 1525 and 1527 cm^{-1} (amide II), for SF hydrogels formed after 7 d of dialysis subjected to freezing or not (**Fig. 2C and D**, respectively), is also attributed to the SF silk II structural conformation.[32-34] The adsorption band at 1234 cm^{-1} (amide III), for both SF hydrogels formed after 7 d of dialysis is ascribed as silk I structural conformation.[35]

In all the analyzed hydrogels the co-existence of silk I and silk II conformations was observed, which is typical of SF hydrogels.

Thermal analysis

Thermogravimetric curves of SF hydrogels are shown in **Figure 3**. The thermograms of all samples showed similar trend. The initial weight loss of SF hydrogels at around 100 °C is due to loss of water. The second weight loss took place within the temperature range between 270 and 380 °C and is associated with the breakdown of side chain groups of amino acid residues as well as the cleavage of peptide bonds.[37,38]

For observation of SF hydrogels degradation peaks, derivate of the thermogravimetric curves were analyzed, as shown in **Figure 4**. It is possible to observe that all samples presented similar behavior, with a peak at around 330–340 °C, which is attributed to the thermal degradation of SF hydrogels.

Morphology

Figure 5 shows the micrographs of the SF hydrogels porous structure obtained by SEM. These revealed that all samples had 3D morphologies with uniform porous structures and they showed the effect of freezing on SF hydrogels formed at 37 °C after 3 d of dialysis (**Fig. 5A**) and SF hydrogels formed after 7 d of dialysis (**Fig. 5C**), which were frozen at -20 °C for 24 h, compared with the SF hydrogels kept at 8 °C (**Fig. 5B and D**). The SF hydrogels subjected to freezing presented a pore size much larger than the hydrogels kept at 8 °C. Moreover, it is possible to see that the SF hydrogels formed after 7 d of dialysis kept at 8 °C showed a thicker fibroin network with smaller pores (**Fig. 5D**) than SF hydrogels formed after 3 d of dialysis (**Fig. 5B**).

Discussion

Significant work has been performed over the last decade to develop natural polymers for biomedical applications, particularly for biocompatible implantable materials.[39] Among natural polymers, silk is an interesting candidate component for tissue engineering. The goal of this research was to study the role of dialysis and freezing on structural conformation, thermal properties and morphology of silk fibroin hydrogels.

The SF solution, before dialysis, is supersaturated and can be stored without undergoing gelation for several months. This happens due to the high ionic strength that promotes SF fibers solvation. During the dialysis, the salt ions diffuse from SF solution into the dialysis water and the ionic force decreases. This allows more interaction between SF molecules and the solution may undergo a sol-gel transition.[19]

Through X-ray diffraction measurement, some information about SF crystalline structure and its conformations of silk I and silk II can be obtained from its crystal structure transition. The distinct halos found in the X-ray diffractograms at $2\theta = 20.4°$,

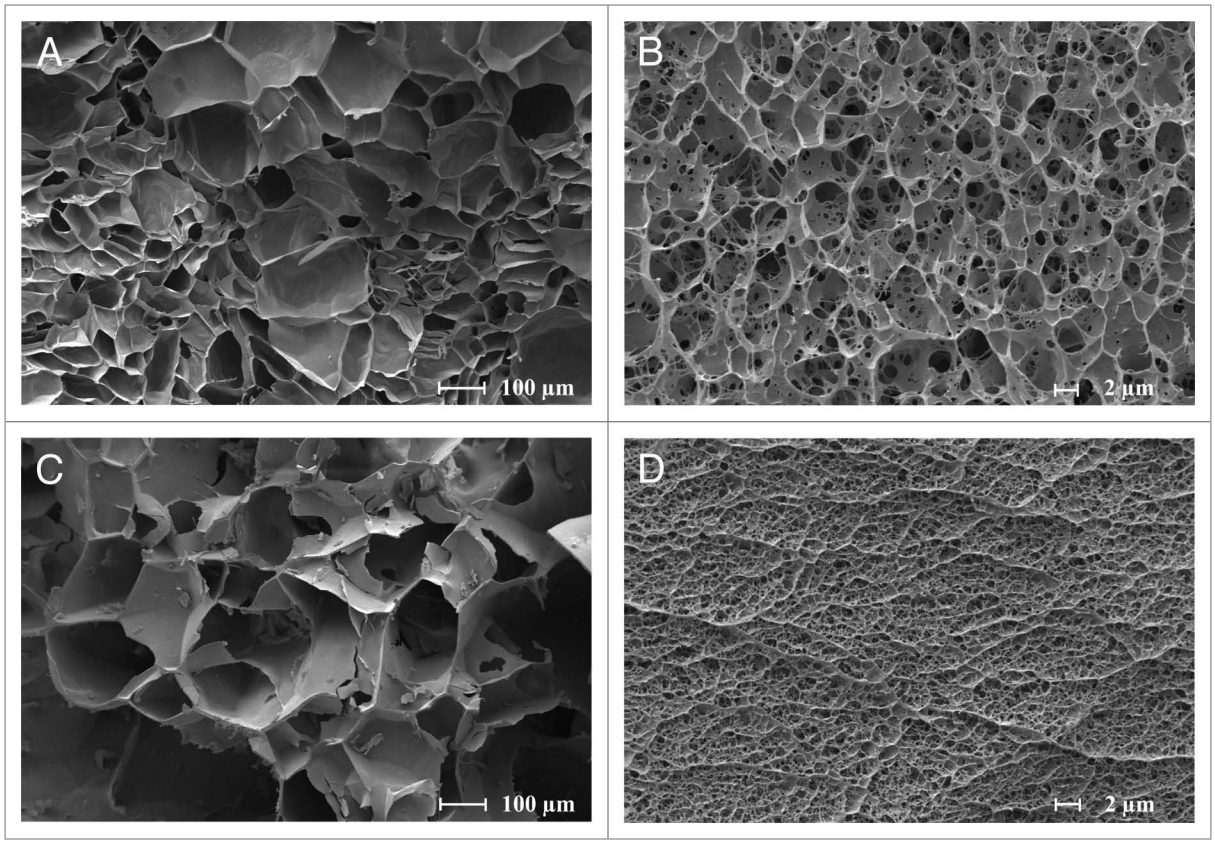

Figure 5. SEM micrographs of the porous structure SF hydrogels formed at 37 °C after 3 d of dialysis subjected to freezing (**A**) or kept at 8 °C (**B**) and SF hydrogels formed after 7 d of dialysis subjected to freezing (**C**) or kept at 8 °C (**D**).

2θ = 20.2°, 2θ = 20.7° and 2θ = 20.6° for SF hydrogels presented typical patterns of β-sheet structure (silk II). Previous studies by Kim et al. presented that all hydrogels prepared in your work showed a distinct halo at 2θ = 20.6°, which is attributed to β-sheet crystalline structure of SF.[14] Kundu et al. observed a halo at 2θ = 20.2° denoting the silk II structure appeared in the XRD pattern of the SF nanoparticles made from *B. mori* protein.[20] Kim et al. observed a halo at 2θ = 20.4° for SF scaffolds indicating that is a β-sheet crystalline structure (silk II).[28] Lv et al. showed the presence of the diffraction halo at 2θ = 20.7° in silk fibroin films, corresponding to β-sheet structure.[30] This β-sheet conformation is formed during SF solution gelation, as a result of SF molecular chain dehydration and their intra and intermolecular hydrogen bond formations. In solution, SF molecules are predominantly organized into the α-helix and random coil structure. However, this structure tends to convert to the β-sheet upon hydrogel formation, which is thermodynamically more stable.[40] No remarkable differences were observed in the XRD spectra of the SF hydrogels formed under different conditions within this study.

FTIR spectroscopy is very sensitive to conformational modifications of silk fibroin. Each SF crystalline form shows a specific absorption band in distinct vibrational regions associated with the amide groups in proteins. The more interesting infrared bands to analyze proteins are the amide bands: amide I, amide II and amide III.[31] Results of FTIR investigation showed that there were slight shifts of the adsorption bands of amides but without conformational changes. This indicates that SF presented in the hydrogel is highly stable and does not change its conformation due to changes in external factors.

Thermal decomposition of SF is mainly influenced by the intrinsic morphological and physical properties of the protein.[41,42] The results obtained by TGA suggest that SF hydrogels thermal degradation occurs at 330–340 °C, which according to the literature is related to SF materials with crystalline β-sheet (silk II) conformation.[42,43] This result is in agreement with the XRD result, which determined that the secondary structure of SF hydrogels is predominantly β-sheet (silk II). By FTIR analysis was possible to verify the presence of silk I conformation on the amide III absorption band, indicating that this structure may occur in the fibroin hydrogels, but in a lower proportion when compared with the silk II.

Morphology of SF hydrogels, reveled by SEM micrographs, indicates the presence of a porous structure with three-dimensional interconnectivity.[14,43-47] The SF hydrogels subjected to freezing (–20 °C) showed larger pore size when compared with SF hydrogels kept at 8 °C. The SF hydrogels kept at 8 °C were frozen with liquid nitrogen before the lyophilization. In the lyophilization procedure, pore size of the material is controlled by the size of the ice crystals formed during freezing. The freezing process with liquid nitrogen is particularly rapid and, ideally, the water presented within the pores of the hydrogel turns into ice crystals that sublimate during lyophilization, maintaining the

same shape and size of the pores of the hydrogel. However, when the freezing process is performed at a higher temperature, such as freezing at –20 °C, ice nucleation is slow and the nuclei tend to grow into larger ice crystals, which leads to the generation of materials with large and random pores.[48] The porous features resulting from freezing are in good agreement with precise results. Guan et al. showed that when polyurethane scaffolds were frozen in liquid nitrogen small pores were observed and most of the pores were less than 10 μm in size.[49] Chun et al. observed that the pore size of porous poly(D,L-lactic-co-glycolic acid) scaffolds frozen at liquid nitrogen temperature was smaller than 5 μm, but the pore size was enlarged up to 30–50 μm when frozen at –20 °C for 24 h.[50] Similarly, Ma et al. observed that when the temperature was decreased from –20 °C to –196 °C (liquid nitrogen) the pore size of poly(L -lactic acid) scaffolds was greatly decreased from 115–140 μm to 20–40 μm.[51] Chung et al. also showed that the pores of alginate/galactosylated chitosan scaffolds formed after liquid nitrogen treatment were small than the pores formed after freezing at –20 °C and –70 °C.[52]

Other processes for the preparation of porous materials include: solvent casting/particulate leaching,[38] emulsion templating[39] and phase separation.[40] In general, these methods require the use of large amounts of organic solvents and a lengthy washing or etching procedure.[38,42,43] A freezing process can provide certain advantages over the traditionally used techniques cited above.[44] Water is an environment-friendly solvent and the use of ice crystals as porogens is green and sustainable. This is particularly beneficial for biological applications. When removing the solvent, the freezing process does not bring impurities into the samples and a further purifying process is therefore not necessary.

Materials and Methods

Preparation of silk fibroin solution

Cocoons of *Bombyx mori* silkworm were supplied by Bratac. To obtain pure SF fibers from silkworm cocoons it was necessary to perform a degumming process of silk cocoons to remove the sericin coating. This process was achieved by initially washing the cocoons with distilled water to remove any impurity, followed by the immersion of cocoons in 1 g/L of Na_2CO_3 solution at 85 °C for 1 h and 30 min, with solution change every 30 min. A final wash in distilled water was done to remove Na_2CO_3 residues. The SF fibers were dried and dissolved in a ternary solvent of $CaCl_2$:CH_3CH_2OH:H_2O, in a molar ratio of 1:2:8, at 85 °C until total dissolution, to a SF salt solution of 10% (w/v).[17]

Preparation of fibroin hydrogels

We studied two different methods for the preparation of fibroin hydrogels. In the first method, SF solution at a concentration of 10% (w/v) was dialyzed (cellulose membrane, Viscofan 22 EU – 20 USA) against distilled water for 3 d, at 8 °C, with water change every 24 h. After dialysis, the solution was filtered by gauze to remove small amounts of aggregates. The final concentration of the silk fibroin aqueous solution was 4% (w/v), which was determined by weighing the remaining solid after drying. The dialyzed solution was placed on specific molds (diameter: 25 mm) in a thermostatic bath at 37 °C until the formation of gels (3 d). Hydrogel formation was observed when the sample presented an opaque white color and did not fall when the mold was inverted for 30s.[14,53] Cylinder-shaped samples sized 25 mm in diameter and 10 mm in thickness were used. The SF hydrogels were then subjected to a freezing at -20 °C for 24 h. To analyze the effect of freezing, control samples of SF hydrogels were kept at 8 °C for 24 h.

In the second method, SF salt solution in a concentration of 10% (w/v) was dialyzed (cellulose membrane, Viscofan 22 EU – 20 USA) against distilled water at 8 °C, with water change every 24 h, until the formation of hydrogels inside the dialysis tube (7 d). The influence of freezing on this hydrogels was also analyzed by freezing SF hydrogels at -20 °C for 24 h, while the control samples (non-frozen hydrogels) were kept at 8 °C for 24 h.

Four different types of samples were prepared: 1) dialysis for 3 d followed by hydrogel formation at 37 °C and freezing by 24h at -20 °C; 2) dialysis for 3 d followed by hydrogel formation at 37 °C and kept at 8 °C for 24 h; 3) dialysis for 7 d until hydrogel formation inside the tube and freezing by 24h at -20 °C and 4) dialysis for 7 d until hydrogel formation inside the tube and kept at 8 °C for 24h.

All hydrogels were characterized after freezing by liquid nitrogen and lyophilization (Liobras, L101, Brazil) within the first 24 h to prevent structural changes.

Characterization

X-ray Diffraction

Changes in the crystallinity of hydrogels were followed with X-ray diffraction (XRD), performed by a X'Pert-MPD diffractometer (Philips Analytical X Ray) with Cu-Kα radiation, with a wavelength of 1.54 Å. The X-ray source was operated at 40 kV and 40 pA. The scanning speed was 0.06°/s, step size of 0.02°, and the measurement range was 2θ = 10–40°. Three samples were used for each type of material.

Fourier Transformed Infrared Spectroscopy

The structural changes of silk fibroin hydrogels were analyzed in the range of 675–4000 cm^{-1}, with a resolution of 4 cm^{-1}, using Fourier transformed infrared spectroscopy with attenuated total reflection apparatus (FTIR-ATR) (Nicolet 6700, Thermo Scientific). FTIR was used to identify the secondary structure of the protein samples through the location of the peaks of amide I, II and III. Three samples were used for each type of material.

Thermogravimetric Analysis

Thermogravimetric analysis (TGA) measurements were performed on the hydrogels using a thermogravimetric analyzer (TGA-50, Shimadzu) in the temperature range of 30–600 °C with a slope of 10 °C/min and a N_2 flow of 50 mL/min, in order to analyze the influence of dialysis and freezing on the weight loss of the samples with respect to the temperature. Three samples were used per each type of material.

Scanning Electron Microscopy

The cross-section morphology of fibroin hydrogels was observed by scanning electron microscopy (SEM). The analysis was performed on the lyophized samples coated with a gold layer and then examined with an EVO MA15 scanning electron

microscope (Zeiss), at 200× and 5000× magnification, with an accelerating voltage of 10 kV.

Conclusions

The present work describes the formation and characterization of silk fibroin hydrogels. Three-dimensional silk fibroin hydrogels were successfully prepared with an interconnected porous structure. From the results of X-ray diffraction and FTIR-ATR analysis, it is concluded that SF transforms into β-sheet after gelation, and both silk I and silk II structures exist simultaneously in all hydrogels. Thermal analysis showed the degradation peak for all SF hydrogels at around 330–340 °C, indicating high thermal resistance for these hydrogels. Longer dialysis time (7 d) resulted in a thicker fibroin network after lyophilization, showing that the dialysis time has an effect on the material porous structure and morphology. The effect of freezing was also visible on the porous structure of SF hydrogels, considerably increasing pore sizes. These scaffolds may hold promise in bone tissue engineering, and the degradation rate of the SF porous structures and in vitro citocompatibility tests are subject of future work.

Disclosure of Potential Conflicts of Interest

No potential conflicts of interest were disclosed.

Acknowledgments

This work was financed by FEDER funds through the Programa Operacional Factores de Competitividade – COMPETE and by Portuguese funds through FCT – Fundação para a Ciência e a Tecnologia in the framework of the NaNOBiofilm project (PTDC/SAUBMA/111233/2009) and PhD grant (SFRH/BD/90400/2012), whose support is acknowledged. The support of Project 346/13 CAPES (Brazil)-FCT (Portugal) Call 21/2012, and CNPq (Brazil) is acknowledged.

References

1. Deville S, Saiz E, Tomsia AP. Freeze casting of hydroxyapatite scaffolds for bone tissue engineering. Biomaterials 2006; 27:5480-9; PMID:16857254; http://dx.doi.org/10.1016/j.biomaterials.2006.06.028
2. Turco G, Marsich E, Bellomo F, Semeraro S, Donati I, Brun F, Grandolfo M, Accardo A, Paoletti S. Alginate/Hydroxyapatite biocomposite for bone ingrowth: a trabecular structure with high and isotropic connectivity. Biomacromolecules 2009; 10:1575-83; PMID:19348419; http://dx.doi.org/10.1021/bm900154b
3. Liu C, Xia Z, Czernuszka JT. Design and development of three-dimensional scaffolds for tissue engineering. Chem Eng Res Des 2007; 85:1051-64; http://dx.doi.org/10.1205/cherd06196
4. Altman GH, Diaz F, Jakuba C, Calabro T, Horan RL, Chen J, Lu H, Richmond J, Kaplan DL. Silk-based biomaterials. Biomaterials 2003; 24:401-16; PMID:12423595; http://dx.doi.org/10.1016/S0142-9612(02)00353-8
5. Vepari C, Kaplan DL. Silk as a Biomaterial. Prog Polym Sci 2007; 32:991-1007; PMID:19543442; http://dx.doi.org/10.1016/j.progpolymsci.2007.05.013
6. Wang Y, Kim HJ, Vunjak-Novakovic G, Kaplan DL. Stem cell-based tissue engineering with silk biomaterials. Biomaterials 2006; 27:6064-82; PMID:16890988; http://dx.doi.org/10.1016/j.biomaterials.2006.07.008
7. Kurioka A, Yamazaki M, Hirano H. Primary structure and possible functions of a trypsin inhibitor of Bombyx mori. Eur J Biochem 1999; 259:120-6; PMID:9914483; http://dx.doi.org/10.1046/j.1432-1327.1999.00030.x
8. Takahashi M, Tsujimoto K, Yamada H, Takagi H, Nakamori S. The silk protein, sericin, protects against cell death caused by acute serum deprivation in insect cell culture. Biotechnol Lett 2003; 25:1805-9; PMID:14677702; http://dx.doi.org/10.1023/A:1026284620236
9. Altman GH, Horan RL, Lu HH, Moreau J, Martin I, Richmond JC, Kaplan DL. Silk matrix for tissue engineered anterior cruciate ligaments. Biomaterials 2002; 23:4131-41; PMID:12182315; http://dx.doi.org/10.1016/S0142-9612(02)00156-4
10. Bayraktar O, Malay O, Özgarip Y, Batigün A. Silk fibroin as a novel coating material for controlled release of theophylline. Eur J Pharm Biopharm 2005; 60:373-81; PMID:15996578; http://dx.doi.org/10.1016/j.ejpb.2005.02.002
11. Gobin AS, Butler CE, Mathur AB. Repair and regeneration of the abdominal wall musculofascial defect using silk fibroin-chitosan blend. Tissue Eng 2006; 12:3383-94; PMID:17518675; http://dx.doi.org/10.1089/ten.2006.12.3383
12. Wang Y, Kim HJ, Vunjak-Novakovic G, Kaplan DL. Stem cell-based tissue engineering with silk biomaterials. Biomaterials 2006; 27:6064-82; PMID:16890988; http://dx.doi.org/10.1016/j.biomaterials.2006.07.008
13. Li C, Vepari C, Jin HJ, Kim HJ, Kaplan DL. Electrospun silk-BMP-2 scaffolds for bone tissue engineering. Biomaterials 2006; 27:3115-24; PMID:16458961; http://dx.doi.org/10.1016/j.biomaterials.2006.01.022
14. Kim UJ, Park J, Li C, Jin HJ, Valluzzi R, Kaplan DL. Structure and properties of silk hydrogels. Biomacromolecules 2004; 5:786-92; PMID:15132662; http://dx.doi.org/10.1021/bm0345460
15. Asakura T, Yao J, Yamane T, Umemura K, Ulrich AS. Heterogeneous structure of silk fibers from Bombyx mori resolved by 13C solid-state NMR spectroscopy. J Am Chem Soc 2002; 124:8794-5; PMID:12137522; http://dx.doi.org/10.1021/ja020244e
16. Kawahara Y, Furukawa K, Yamamoto T. Self-expansion behavior of silk fibroin film. Macromol Mater Eng 2006; 291:458-62; http://dx.doi.org/10.1002/mame.200500350
17. de Moraes MA, Nogueira GM, Weska RF, Beppu MM. Preparation and Characterization of Insoluble Silk Fibroin/Chitosan Blend Films. Polymers 2010; 2:719-27; http://dx.doi.org/10.3390/polym2040719
18. Sashina ES, Bochek AM, Novoselov NP, Kirichenko DA. Structure and solubility of natural silk fibroin. Russ J Appl Chem 2006; 79:869-76; http://dx.doi.org/10.1134/S1070427206060012
19. Nogueira GM, de Moraes MA, Rodas ACD, Higa OZ, Beppu MM. Hydrogels from silk fibroin metastable solution: Formation and characterization from a biomaterial perspective. Mat Sci Eng C-Mater 2011; 31:997-1001; http://dx.doi.org/10.1016/j.msec.2011.02.019
20. Kundu J, Chung YI, Kim YH, Tae G, Kundu SC. Silk fibroin nanoparticles for cellular uptake and control release. Int J Pharm 2010; 388:242-50; PMID:20060449; http://dx.doi.org/10.1016/j.ijpharm.2009.12.052
21. Wang X, Kluge JA, Leisk GG, Kaplan DL. Sonication-induced gelation of silk fibroin for cell encapsulation. Biomaterials 2008; 29:1054-64; PMID:18031805; http://dx.doi.org/10.1016/j.biomaterials.2007.11.003
22. Wang T, Zhang LL, He XJ. Preparation and Characterization of a Novel Hybrid Hydrogel Composed of Bombyx mori Fibroin and Poly (N-isopropylacrylamide). J Nanomater 2013;2013; http://dx.doi.org/10.1155/2013/832710
23. Hardy JG, Scheibel TR. Composite materials based on silk proteins. Prog Polym Sci 2010; 35:1093-115; http://dx.doi.org/10.1016/j.progpolymsci.2010.04.005
24. Mandal BB, Kundu SC. Non-bioengineered silk fibroin protein 3D scaffolds for potential biotechnological and tissue engineering applications. Macromol Biosci 2008; 8:807-18; PMID:18702171; http://dx.doi.org/10.1002/mabi.200800113
25. Ren L, Tsuru K, Hayakawa S, Osaka A. Novel approach to fabricate porous gelatin-siloxane hybrids for bone tissue engineering. Biomaterials 2002; 23:4765-73; PMID:12361615; http://dx.doi.org/10.1016/S0142-9612(02)00226-0
26. Fukasawa T, Deng ZY, Ando M, Ohji T, Goto Y. Pore structure of porous ceramics synthesized from water-based slurry by freeze-dry process. J Mater Sci 2001; 36:2523-7; http://dx.doi.org/10.1023/A:1017946518955
27. Zhang H, Cooper AI. Aligned porous structures by directional freezing. Adv Mater 2007; 19:1529-33; http://dx.doi.org/10.1002/adma.200700154
28. Kim UJ, Park J, Kim HJ, Wada M, Kaplan DL. Three-dimensional aqueous-derived biomaterial scaffolds from silk fibroin. Biomaterials 2005; 26:2775-85; PMID:15585282; http://dx.doi.org/10.1016/j.biomaterials.2004.07.044
29. Wang H, Zhang Y, Shao H, Hu X. A study on the flow stability of regenerated silk fibroin aqueous solution. Int J Biol Macromol 2005; 36:66-70; PMID:15916801; http://dx.doi.org/10.1016/j.ijbiomac.2005.03.011
30. Lv Q, Cao C, Zhu H. Clotting times and tensile properties of insoluble silk fibroin films containing heparin. Polym Int 2005; 54:1076-81; http://dx.doi.org/10.1002/pi.1814
31. Rusa CC, Bridges C, Ha SW, Tonelli AE. Conformational changes induced in Bombyx mori silk fibroin by cyclodextrin inclusion complexation. Macromolecules 2005; 38:5640-6; http://dx.doi.org/10.1021/ma050340a
32. Hu X, Shmelev K, Sun L, Gil ES, Park SH, Cebe P, Kaplan DL. Regulation of silk material structure by temperature-controlled water vapor annealing. Biomacromolecules 2011; 12:1686-96; PMID:21425769; http://dx.doi.org/10.1021/bm200062a

33. Hu X, Kaplan D, Cebe P. Determining Beta-Sheet Crystallinity in Fibrous Proteins by Thermal Analysis and Infrared Spectroscopy. Macromolecules 2006; 39:6161-70; http://dx.doi.org/10.1021/ma0610109
34. Lu Q, Hu X, Wang X, Kluge JA, Lu S, Cebe P, Kaplan DL. Water-insoluble silk films with silk I structure. Acta Biomater 2010; 6:1380-7; PMID:19874919; http://dx.doi.org/10.1016/j.actbio.2009.10.041
35. Srisa-Ard M, Baimark Y. Controlling Conformational Transition of Silk Fibroin Microspheres by Water Vapor for Controlled Release Drug Delivery. Particul Sci Technol 2013; 31:379-84; http://dx.doi.org/10.1080/02726351.2013.766289
36. Kweon HY, Park SH, Ye JH, Lee YW, Cho CS. Preparation of semi-interpenetrating polymer networks composed of silk fibroin and poly(ethylene glycol) macromer. J Appl Polym Sci 2001; 80:1848-53; http://dx.doi.org/10.1002/app.1281
37. Um IC, Kweon HY, Park YH, Hudson S. Structural characteristics and properties of the regenerated silk fibroin prepared from formic acid. Int J Biol Macromol 2001; 29:91-7; PMID:11518580; http://dx.doi.org/10.1016/S0141-8130(01)00159-3
38. Nogueira GM, Weska RF, Vieira WC, Polakiewicz B, Rodas ACD, Higa OZ, et al. A New Method to Prepare Porous Silk Fibroin Membranes Suitable for Tissue Scaffolding Applications. J Appl Polym Sci 2009; 114:617-23; http://dx.doi.org/10.1002/app.30627
39. Malafaya PB, Silva GA, Reis RL. Natural-origin polymers as carriers and scaffolds for biomolecules and cell delivery in tissue engineering applications. Adv Drug Deliv Rev 2007; 59:207-33; PMID:17482309; http://dx.doi.org/10.1016/j.addr.2007.03.012
40. Matsumoto A, Chen J, Collette AL, Kim UJ, Altman GH, Cebe P, Kaplan DL. Mechanisms of silk fibroin sol-gel transitions. J Phys Chem B 2006; 110:21630-8; PMID:17064118; http://dx.doi.org/10.1021/jp056350v
41. Tsukada M, Obo M, Kato H, Freddi G, Zanetti F. Structure and dyeability of Bombyx mori silk fibers with different filament sizes. J Appl Polym Sci 1996; 60:1619-27; http://dx.doi.org/10.1002/(SICI)1097-4628(19960606)60:10<1619::AID-APP14>3.0.CO;2-#
42. Freddi G, Pessina G, Tsukada M. Swelling and dissolution of silk fibroin (Bombyx mori) in N-methyl morpholine N-oxide. Int J Biol Macromol 1999; 24:251-63; PMID:10342772; http://dx.doi.org/10.1016/S0141-8130(98)00087-7
43. Fang JY, Chen JP, Leu YL, Wang HY. Characterization and evaluation of silk protein hydrogels for drug delivery. Chem Pharm Bull (Tokyo) 2006; 54:156-62; PMID:16462057; http://dx.doi.org/10.1248/cpb.54.156
44. Nazarov R, Jin HJ, Kaplan DL. Porous 3-D scaffolds from regenerated silk fibroin. Biomacromolecules 2004; 5:718-26; PMID:15132652; http://dx.doi.org/10.1021/bm034327e
45. Zhu Y, Wan Y, Zhang J, Yin D, Cheng W. Manufacture of layered collagen/chitosan-polycaprolactone scaffolds with biomimetic microarchitecture. Colloids Surf B Biointerfaces 2014; 113:352-60; PMID:24121078; http://dx.doi.org/10.1016/j.colsurfb.2013.09.028
46. Han J, Zhou Z, Yin R, Yang D, Nie J. Alginate-chitosan/hydroxyapatite polyelectrolyte complex porous scaffolds: preparation and characterization. Int J Biol Macromol 2010; 46:199-205; PMID:19941890; http://dx.doi.org/10.1016/j.ijbiomac.2009.11.004
47. Sarem M, Moztarzadeh F, Mozafari M, Shastri VP. Optimization strategies on the structural modeling of gelatin/chitosan scaffolds to mimic human meniscus tissue. Mater Sci Eng C Mater Biol Appl 2013; 33:4777-85; PMID:24094187; http://dx.doi.org/10.1016/j.msec.2013.07.036
48. Qian L, Zhang HF. Controlled freezing and freeze drying: a versatile route for porous and micro-/nano-structured materials. J Chem Technol Biotechnol 2011; 86:172-84; http://dx.doi.org/10.1002/jctb.2495
49. Guan J, Fujimoto KL, Sacks MS, Wagner WR. Preparation and characterization of highly porous, biodegradable polyurethane scaffolds for soft tissue applications. Biomaterials 2005; 26:3961-71; PMID:15626443; http://dx.doi.org/10.1016/j.biomaterials.2004.10.018
50. Chun KW, Cho KC, Kim SH, Jeong JH, Park TG. Controlled release of plasmid DNA from biodegradable scaffolds fabricated using a thermally-induced phase-separation method. J Biomater Sci Polym Ed 2004; 15:1341-53; PMID:15648567; http://dx.doi.org/10.1163/1568562042368103
51. Ma H, Hu J, Ma PX. Polymer scaffolds for small-diameter vascular tissue engineering. Adv Funct Mater 2010; 20:2833-41; PMID:24501590; http://dx.doi.org/10.1002/adfm.201000922
52. Chung TW, Yang J, Akaike T, Cho KY, Nah JW, Kim SI, Cho CS. Preparation of alginate/galactosylated chitosan scaffold for hepatocyte attachment. Biomaterials 2002; 23:2827-34; PMID:12069321; http://dx.doi.org/10.1016/S0142-9612(01)00399-4
53. Liu Y, Cheng YD, Xiong SY, Li PJ, Wei YQ, Li MZ. The Effect of Shearing Force on the Gel Formation and Structural Transitions of Regenerated Silk Fibroin. Text Bioeng Inform S 2010:309-15.